0026-895X/98/061120-11$3.00/0

MOLECULAR PHARMACOLOGY, **53:**1120–1130 (1998).

On the Unique Binding and Activating Properties of Xanomeline at the M_1 Muscarinic Acetylcholine Receptor

ARTHUR CHRISTOPOULOS, TRACIE L. PIERCE, JENNIFER L. SORMAN, and ESAM E. EL-FAKAHANY

Division of Neuroscience Research in Psychiatry (A.C., J.L.S., E.E.E.) and Department of Cell Biology and Neuroanatomy (T.L.P.), University of Minnesota Medical School, Minneapolis, Minnesota 55455

Received November 14, 1997; Accepted February 23, 1998

This paper is available online at http://www.molpharm.org

ABSTRACT

We investigated the molecular nature of the interaction between the functionally selective M_1 muscarinic acetylcholine receptor (mAChR) agonist xanomeline and the human M_1 mAChR expressed in Chinese hamster ovary (CHO) cells. In contrast to the non-subtype-selective agonist carbachol, xanomeline demonstrated M_1 mAChR binding that was resistant to extensive washout, resulting in a significant reduction in apparent *N*-[^{3}H]methylscopolamine saturation binding affinity in intact cells. Functional assays, using both M_1 mAChR-mediated phosphoinositide hydrolysis and activation of neuronal nitric oxide synthase, confirmed that this persistent binding resulted in elevated basal levels of system activity. Furthermore, this phenomenon could be reversed by the addition of the antagonist atropine. However, pharmacological analysis of the inhibition by atropine of xanomeline-mediated functional responses indicated a possible element of noncompetitive behavior that was not evident in several kinetic and equilibrium binding experimental paradigms. Taken together, our findings indicate for the first time a novel mode of interaction between an mAChR agonist and the M_1 mAChR, which may involve unusually avid binding of xanomeline to the receptor. This yields a fraction of added agonist that is retained at the level of the receptor compartment to persistently bind to and activate the receptor subsequent to washout. The results of the current study suggest that elucidation of the mechanism or mechanisms of interaction of xanomeline with the M_1 mAChR is particularly important in relation to the potential therapeutic use of this agent in the treatment of Alzheimer's disease.

A significant portion of the ongoing research efforts into the treatment of Alzheimer's disease has been devoted to the attempted restoration of central cholinergic function (Giacobini, 1992). This is primarily due to the impressive body of evidence pointing to a consistent loss of presynaptic cholinergic markers, such as choline acetyltransferase and M_2 mAChRs, associated with the disorder (Mash *et al*., 1985; Quirion *et al*., 1989). Although the functional properties of postsynaptic M_1 mAChRs, which are involved in learning and memory, also have been shown to be affected during the progression of the disorder (Ferrari-Dileo *et al*., 1995; Ladner *et al*., 1995), overall postsynaptic receptor numbers are not (Ferrari-Dileo *et al*., 1995).

Consequently, many of the pharmacotherapeutic agents spawned as a result of the cholinergic hypothesis of dementia have consisted of either acetylcholinesterase inhibitors or directly acting mAChR agonists (Giacobini, 1992) in an attempt to exploit any residual M_1 mAChR functionality. Xanomeline (Fig. 1) is a novel member of the latter class of drugs and has been identified as both highly potent and functionally M_1 selective (Shannon *et al*., 1994). Clinical studies that used this agent have revealed a significant improvement in the cognitive function of patients with Alzheimer's disease (Bodick *et al*., 1997). Because xanomeline represents one of the most potent M_1 mAChR agonists known to date (Shannon *et al*., 1994), the current study was undertaken to delineate further the molecular mechanisms behind the potency and functional selectivity of this compound. In particular, the possibility of a unique mode of mAChR activation by xanomeline, which is not common to classic mAChR ligands, was investigated both functionally and in binding studies. Our results demonstrate that xanomeline is able to bind to and activate the M_1 mAChR in a persistent manner and that this mode of interaction is different from that used by conventional agonists such as CCh. A preliminary report of the persistent M_1 mAChR-activating ability of xanomeline was made recently (Christopoulos and El-Fakahany, 1997).

Experimental Procedures

Materials. [^{3}H]NMS (84.5 Ci/mmol) and L-[^{14}C]citrulline (50 mCi/mmol) were purchased from DuPont-New England Nuclear (Boston,

This work was supported by National Institutes of Health Grant NS25743.

ABBREVIATIONS: mAChR, muscarinic acetylcholine receptor; CHO, Chinese hamster ovary; CCh, carbachol; NMS, *N*-methylscopolamine; HEPES, 4-(2-hydroxyethyl)-1-piperazineethanesulfonic acid; PI, phosphoinositide; nNOS, neuronal nitric oxide synthase; DMEM, Dulbecco's modified Eagle's medium; dpm, disintegrations per minute; ANOVA, analysis of variance.

MA). *myo*-[^{3}H]Inositol (107 mCi/mmol) and L-[^{3}H]arginine (64 Ci/mmol) were purchased from Amersham Life Science (Arlington Heights, IL). [^{14}C]Inositol-1-phosphate (300 mCi/mmol) was purchased from American Radiolabeled Chemicals (St. Louis, MO). DMEM was purchased from GIBCO BRL (Gaithersburg, MD). Geneticin and hygromycin were purchased from Calbiochem (La Jolla, CA). Bovine calf serum was purchased from Hyclone (Logan, UT). Xanomeline tartrate was a generous gift from Lilly Research Laboratories (Indianapolis, IN). All other reagents were purchased from Sigma Chemical (St. Louis, MO).

Cell culture. CHO cells, stably expressing the human M_1 mAChR (CHO hm1 cells), were kindly provided by Dr. M. Brann (University of Vermont Medical School, Burlington, VT) and were grown for 4 days at 37° in DMEM supplemented with 10% bovine calf serum and 50 μg/ml geneticin in a humidified atmosphere consisting of 5% CO_2/95% air. CHO cells stably expressing both the M_1 mAChR and nNOS (CHO hm1/nNOS cells) were grown under similar conditions but in the additional presence of hygromycin (50 μg/ml). The cDNA encoding nNOS was kindly provided by Drs. S. H. Snyder and D. R. Bredt (The Johns Hopkins University School of Medicine, Baltimore, MD). Cells were used 4 days after subculturing and were harvested by trypsinization followed by centrifugation (300 × g, 3 min) and resuspension of the pellet in HEPES buffer (110 mM NaCl, 5.4 mM KCl, 1.8 mM $CaCl_2$, 1 mM $MgSO_4$, 25 mM glucose, 50 mM HEPES, 58 mM sucrose; pH 7.4 ± 0.02; 340 ± 5 mOsM), repeated twice.

Assay of nNOS activity. The activity of nNOS in CHO hm1/nNOS cells was assayed by quantifying the conversion of L-[^{3}H]arginine to L-[^{3}H]citrulline according to the method of Bredt and Snyder (1989) with modifications (Wang *et al*., 1994). Subsequent to harvesting and washout, CHO hm1/nNOS cells (~5 × 10^5/tube) were incubated in 0.3 ml of HEPES buffer for 15 min at 37°, after which L-[^{3}H]arginine (0.06 μCi/tube) was added to initiate the reaction. At the same time, increasing concentrations of either CCh or xanomeline were added in the absence or presence of atropine (30 nM) or pirenzepine (150 nM). Antagonists were incubated with the cells for 20 min before the addition of agonist. After 1 hr at 37°, the reaction was stopped with an excess of L-arginine (5 mM) and EDTA (4 mM). L-[^{3}H]Citrulline was separated from L-[^{3}H]arginine using ion exchange chromatography (DOWEX AG50W-X8 resin), and the amount of radioactivity, expressed as dpm, was determined via liquid scintillation counting. In other experiments, the residual effects of xanomeline pretreatment on basal nNOS activity were examined in terms of time dependence, concentration dependence, and reversibility by atropine (10 μM), as outlined in Results. In these latter experiments, the L-[^{3}H]arginine was added subsequent to all washout procedures.

Assay of PI hydrolysis. CHO hm1 cells were suspended in buffer and loaded with *myo*-[^{3}H]inositol (8 μCi/ml) for 1 hr at 37°. Labeled cells were washed with HEPES buffer containing 10 mM LiCl, distributed to assay tubes (~5 × 10^5/tube), and allowed to incubate for 15 min at 37°. Concentration-response curves for the stimulation of PI hydrolysis by either CCh or xanomeline were constructed in the absence or presence of 30 nM atropine. The antagonist was equilibrated with the cells for 20 min before the addition of agonist. To assess agonist-induced desensitization, experiments also were conducted on cells that had been pretreated for 24 hr at 37° with either 1 mM CCh or 1 μM xanomeline before harvesting. With a third experimental protocol, we examined basal PI activity in cells that had been pretreated with either 1 mM CCh or 1 μM xanomeline for 1 hr at 37° before harvesting and washing. In all instances, the reaction was allowed to proceed for 1 hr after the addition of agonist or vehicle control before being stopped with chloroform/methanol (2:1). Tubes were centrifuged (450 × g; 15 min), and total inositol phosphates were separated by ion exchange chromatography on DOWEX AG1-X8 resin, with [^{14}C]inositol-1-phosphate as a recovery standard. The amount of radioactivity (dpm) in each sample then was determined by liquid scintillation counting.

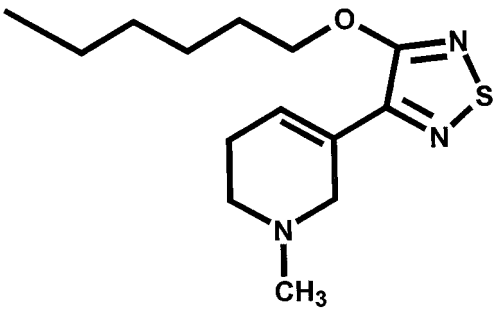

Fig. 1. Structure of xanomeline.

Saturation binding experiments. All radioligand binding experiments used ~10^5 cells/assay tube in a total volume of 1 ml. For the saturation binding assays, three different protocols were used: (1) to determine radioligand binding parameters, cells were incubated with increasing concentrations of [^{3}H]NMS (0.02–2 nM) for 1 hr at 37°; and (2) to assess persistent agonist binding, CHO hm1 cells were incubated for 1 hr at 37° in the absence or presence of either 1 mM CCh or 1 μM xanomeline, followed by centrifugation and resuspension in HEPES buffer (three times), as described above. Subsequently, the cells were incubated with a saturating concentration (2 nM) of [^{3}H]NMS for 1 hr at 37°; (3) to test for pseudoirreversible agonist binding, CHO hm1 cells were incubated for 2.5 hr at 37° with either 2 nM [^{3}H]NMS alone or in combination with either 100 μM CCh or 100 nM xanomeline, with variations in the order of ligand addition. Agonists were added together with, 30 min before, or 30 min after the radioligand. In all instances, nonspecific binding was defined using 10 μM atropine. Additional saturation experiments were conducted on cells that had been pretreated for 1 hr at 37° with 1 μM xanomeline before washout, as above. Protein determinations were performed according to the method of Bradford (1976).

Competition binding experiments. CHO hm1 cells were incubated with a fixed concentration of [^{3}H]NMS (0.2, 0.4, or 2 nM, as described in Results) in the absence or presence of either CCh (0.1 μM to 10 mM), xanomeline (0.1 nM to 20 μM), or atropine (0.1 nM to 2 μM) for 1 hr at 37°. Additional atropine competition experiments were conducted in the presence of both [^{3}H]NMS and a fixed concentration of xanomeline (30 or 100 nM). Nonspecific binding was defined as above.

Dissociation kinetic experiments. CHO hm1 cells were incubated with a fixed concentration of either 0.2 nM [^{3}H]NMS alone or 0.4 nM [^{3}H]NMS together with 30 nM xanomeline for 1 hr at 37°. After this period, 200 nM unlabeled NMS was added, alone or in combination with 1 μM xanomeline, to inhibit radioligand reassociation. Subsequently, the amount of radioactivity was measured at various time intervals to determine the [^{3}H]NMS dissociation rate. Nonspecific binding was defined as above.

For all binding experiments, incubation was terminated by filtration through Whatman GF/C filters (Clifton, NJ), positioned on a Brandell Cell Harvester (Montreal, Quebec, Canada). Filters were washed three times with 4-ml aliquots of ice-cold saline and dried before radioactivity (dpm) was measured using liquid scintillation counting.

Data analysis. Datasets of total and nonspecific binding, derived from each complete saturation binding assay, were simultaneously analyzed via nonlinear regression with Microsoft Excel 5.0 to derive individual estimates of B_{max} (total receptor density) and K_D (radioligand receptor equilibrium dissociation constant). Competition binding isotherms were analyzed via nonlinear regression using Prism 2.01 (GraphPAD Software, San Diego, CA) to derive estimates of n_H (slope factor) and IC_{50} (midpoint location/potency parameter). Assuming simple competition, the data were refitted according to both one- and two-site mass action binding models, and the better model was determined by an extra-sum-of-squares test using Prism.

IC_{50} values were converted to K_I values (competitor receptor equilibrium dissociation constant) according to the equation:

$$K_I = \frac{IC_{50}}{1 + [D]/[K_D] + [B]/[K_B]}$$

where [D] and K_D are the concentration and dissociation constant, respectively, of the radioligand, and [B] and K_B are the concentration and dissociation constant, respectively, of any additional competitor (where applicable). Data from dissociation kinetic experiments were analyzed by Prism according to both monoexponential and biexponential dissociation models and compared by an extra-sum-of-squares test to estimate k_{off}, the radioligand dissociation rate constant.

In the functional assays, individual agonist concentration-response curve data, in the absence and presence of antagonist, were fitted to the four-parameter logistic function (using Prism):

$$E = \text{basal} + \frac{E_{max} \times [A]^{n_H}}{[EC_{50}]^{n_H} + [A]^{n_H}}$$

where E is effect, [A] is the concentration of agonist, n_H is the midpoint slope, EC_{50} is the midpoint location parameter, and E_{max} and basal are the upper and lower asymptotes, respectively. The effect of the antagonist on these parameters was assessed by Student's t test, with values of $p < 0.05$ considered to be significant. If the minimum criteria for competitive antagonism were satisfied (the antagonist produced a parallel, dextral shift of the agonist concentration-response curve with no change in E_{max} and basal), each curve pair was simultaneously analyzed with the program SCIENTIST 2.01 (Micromath Software, Salt Lake City, UT), with E_{max}, n_H, and basal constrained to be shared between curves. In the nNOS assays, it was sometimes possible to obtain only one agonist concentration-response curve per assay per day. Therefore, for each particular series of experiments, a global constrained simultaneous analysis of the entire family of concentration-response curves was performed using SCIENTIST, with standard errors estimated as described elsewhere (Leff *et al.*, 1990). In all cases, values of K_D, IC_{50}, and EC_{50} were estimated as negative logarithms.

Data shown are the mean ± standard error. Comparisons between mean values were made by paired or unpaired t tests or one-way ANOVA, as appropriate. Unless otherwise stated, values of $p < 0.05$ were taken as significant.

Results

Characterization of the concentration-response relationship for xanomeline and CCh in the activation of nNOS and PI hydrolysis. Initial experiments established the concentration-response characteristics of xanomeline- and CCh-mediated responses under standard assay conditions. In terms of nNOS activation, quantified as the conversion of L-[^{3}H]arginine to L-[^{3}H]citrulline, it may be seen from Fig. 2 that xanomeline displayed an intrinsic activity similar to that of the full agonist, CCh. In addition, both agents exhibited a very steep concentration-response relationship, as demonstrated by the large curve slopes, with xanomeline being significantly more potent ($p < 0.05$). Similarly, xanomeline was significantly ($p < 0.05$) more potent than CCh in mediating PI hydrolysis (Fig. 3), with comparable intrinsic activity.

Pharmacological analysis of the antagonism by atropine and pirenzepine of CCh- and xanomeline-mediated activation of nNOS. In subsequent experiments, concentration-response curves to either CCh- or xanomeline-mediated nNOS stimulation were established in the absence and presence of the nonselective antagonist atropine (30 nM) or the M_1-selective antagonist pirenzepine (150 nM). Time course experiments indicated no significant effect of the antagonist on the initial rate of agonist-induced L-[^{3}H]citrulline accumulation (data not shown). The results of the competition experiments are summarized in Fig. 4 and Table 1. The addition of either antagonist did not result in a significant alteration of agonist concentration-response curve parameters ($p > 0.05$), allowing the relative changes in agonist potency to be assessed in terms of a competitive model of pharmacological interaction. Based on the results shown in Fig. 4 and Table 1, atropine and pirenzepine were able to shift the CCh concentration-response curves by factors of ~26- and ~18-fold respectively, whereas for xanomeline, the corresponding shifts were ~20- and ~14-fold, respectively.

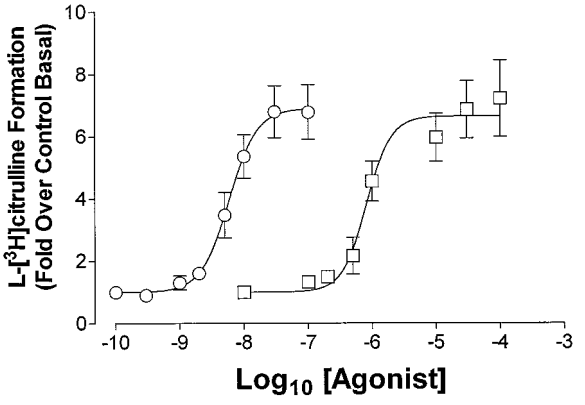

Fig. 2. Concentration-response curves for xanomeline- and CCh-mediated activation of nNOS. CHO hm1/nNOS cells were incubated with increasing concentrations of xanomeline (○) or CCh (□) for 1 hr at 37°. Enzyme activity was assayed by quantifying the conversion of L-[^{3}H]arginine to L-[^{3}H]citrulline. Nonlinear regression analysis yielded these parameters: for xanomeline, maximum over basal = 6.99 ± 0.44, pEC_{50} = 8.23 ± 0.08; n_H = 1.99 ± 0.61; for CCh, maximum over basal = 6.66 ± 0.37, pEC_{50} = 6.08 ± 0.08; n_H = 2.26 ± 0.91. Basal activity in control cells was 4200 ± 600 dpm. Values are mean ± standard error of five independent experiments conducted in triplicate. Where error bars are not shown, they lie within the dimensions of the symbol.

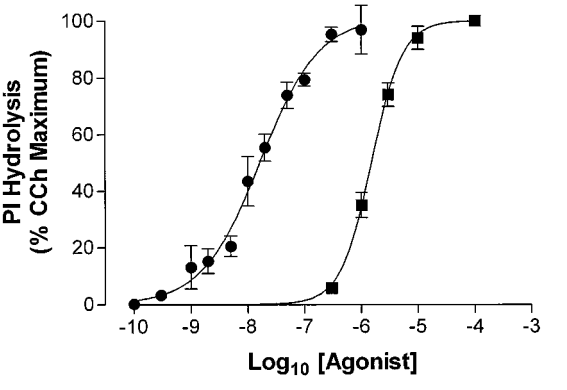

Fig. 3. Concentration-response curves for xanomeline- and CCh-mediated PI hydrolysis. CHO hm1 cells were incubated with increasing concentrations of xanomeline (●) or CCh (■) for 1 hr at 37°. Nonlinear regression analysis yielded these: for xanomeline, percentage of CCh maximum = 101 ± 5%, pEC_{50} = 7.77 ± 0.08; n_H = 0.84 ± 0.09; for CCh, percentage of CCh maximum = 100 ± 2%, pEC_{50} = 5.82 ± 0.03; n_H = 1.58 ± 0.13. Maximal CCh-induced activity in control cells was 7400 ± 1900 dpm. Values are mean ± standard error of four independent experiments conducted in triplicate. Where error bars are not shown, they lie within the dimensions of the symbol.

Pharmacological analysis of the antagonism by atropine of CCh- and xanomeline-mediated PI hydrolysis. Similar experiments were conducted using PI hydrolysis as the biological response and atropine (30 nM) as the antagonist. In contrast to the L-[^{3}H]citrulline assay, significant differences were noted in the ability of atropine to inhibit responses mediated by xanomeline compared with those of CCh. Although the antagonism of the CCh-induced PI response by atropine was compatible with a competitive interaction, characterized by a geometric mean curve shift of ~21-fold, the presence of atropine resulted in a significant ($p < 0.05$) alteration of control xanomeline concentration-response curve slope in addition to midpoint location (Fig. 5, Table 2). The steepening of the concentration-response curve is indicative of an interaction that is not simply competitive. The midpoint location parameters of the xanomeline concentration-response curves were used to derive a geometric mean shift of ~14-fold, although it should be noted that this value may be considered relatively arbitrary because it will be influenced by the lack of parallelism between the two curves. With this caveat in mind, a significant difference ($p < 0.05$) was found between the degree of shift induced by atropine of the concentration-response curve to either agonist.

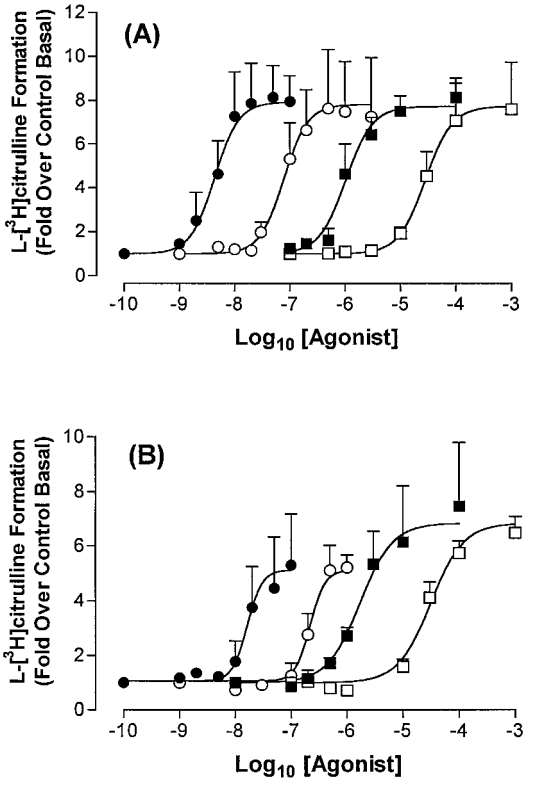

Fig. 4. Inhibition of CCh- and xanomeline-mediated L-[^{3}H]citrulline formation by atropine and pirenzepine in CHO hm1/nNOS cells. Effects of xanomeline (○, ●) or CCh (□, ■) in the absence (●, ■) or presence (○, □) of (A) atropine, 30 nM, and (B) pirenzepine, 150 nM. Cells were equilibrated with antagonist for 20 min at 37° before the addition of agonist or vehicle control for an additional 1 hr. No significant differences ($p > 0.05$) were found between midpoint slopes and maximal asymptotes within each agonist concentration-response curve pair in the absence or presence of antagonist. Values of logistic curve-fitting via nonlinear regression are indicated in Table 1. Values for the basal curve parameter were constrained to 1. Values are (A) mean ± standard error of five independent determinations conducted in triplicate or (B) mean ± standard error of four independent determinations conducted in triplicate. Where error bars are not shown, they lie within the dimensions of the symbol.

TABLE 1

Activation of nNOS in CHO hm1/nNOS cells by CCh or xanomeline

The activity of nNOS was quantified by measuring the formation of L-[^{3}H]citrulline in response to agonist for 1 hr at 37° in HEPES buffer, as indicated in the text. Parameters derived from nonlinear regression analysis are presented as the mean ± standard error of four or five determinations conducted in triplicate. E_{max} and n_H parameter values were constrained to be shared between each pair of agonist curves, in the absence or presence of antagonist (see the text). The basal parameter values were set to 1.

Agonist	Antagonist			
	Atropine (30 nM)		Pirenzepine (150 nM)	
	CCh	Xanomeline	CCh	Xanomeline
E_{max} [a]	7.44 ± 2.04	7.83 ± 2.01	6.85 ± 2.12	5.13 ± 1.91
pEC_{50} (control)	5.96 ± 0.11	8.34 ± 0.14	5.79 ± 0.07	7.79 ± 0.07
pEC_{50} (+antagonist)	4.55 ± 0.13	7.10 ± 0.16	4.53 ± 0.09	6.66 ± 0.08
n_H [b]	1.79 ± 0.57	1.99 ± 1.18	1.47 ± 0.47	3.24 ± 1.89

[a] Expressed as fold-increase over control basal L-[^{3}H]citrulline formation (6200 ± 1470 dpm).

[b] Logistic slope factor. A one-way analysis of variance revealed no difference between any of the values.

Persistent receptor activation by xanomeline; concentration and time dependence. In light of these findings, the possibility of other unique features of the interaction between xanomeline and M_1 mAChR was investigated further. Incubation of CHO hm1/nNOS cells with increasing concentrations of xanomeline (10–100 nM) for 1 hr at 37°, before harvesting and extensive washout, resulted in a progressive increase in basal conversion of L-[^{3}H]arginine to L-[^{3}H]citrulline in the absence of further addition of agonist, as shown in Fig. 6A. Although a trend is evident, a one-way ANOVA detected a significant difference ($p < 0.05$) above basal only for the two highest preincubation concentrations of xanomeline (100 nM and 1 μM). Fig. 6B shows the results of pretreating the cells with 1 μM xanomeline for various times (10–30 min), where differences over basal levels of activity after washing were observed for 10 min of agonist pretreatment, the earliest time point measured.

Effects of CCh and xanomeline pretreatment on PI hydrolysis. Additional functional experiments were undertaken to assess whether the persistent activating effects of

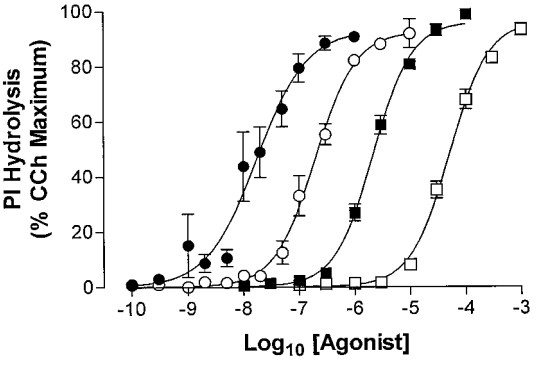

Fig. 5. Inhibition of CCh- and xanomeline-mediated PI hydrolysis by atropine in CHO hm1 cells. Effects of xanomeline (○, ●) or CCh (□, ■) in the absence (●, ■) or presence (○, □) of atropine, 30 nM. Cells were equilibrated with antagonist for 20 min at 37° before the addition of agonist or vehicle control for an additional 1 hr. A significant difference ($p < 0.05$) was found between the midpoint slopes of the xanomeline concentration-response curves obtained in the absence or presence of antagonist. Values of logistic curve-fitting via nonlinear regression are indicated in Table 2. Values for the basal curve parameter were constrained to 0. Values are mean ± standard error of five independent determinations conducted in triplicate. Where error bars are not shown, they lie within the dimensions of the symbol.

xanomeline outlined above were due to an artifact particular to the choice of biological assay that was used. Thus, the ability of M_1 mAChRs to mediate PI hydrolysis was exploited as a second functional experimental paradigm. CHO hm1 cells were pretreated with either 1 mM CCh or 1 μM xanomeline for 1 hr at 37° before washout and harvesting, as above (Fig. 7A). In contrast to CCh, xanomeline pretreatment, followed by washout, resulted in a persistently elevated level of basal PI activity, being ~20-fold greater than control cells pretreated in parallel with vehicle. Xanomeline thus displays a novel, persistent, receptor-activating ability in at least two common functional indicators of M_1 mAChR activation.

In addition, the effects of long term xanomeline pretreatment of CHO hm1 cells were examined (Fig. 7B). Cells were preincubated with either 1 mM CCh or 1 μM xanomeline for 24 hr at 37° and then washed and harvested. Subsequently, full concentration-response curves to CCh were established. In this manner, any changes in lower curve asymptote, upper curve asymptote, midpoint location, and slope may be interpreted as effects of long term agonist treatment on basal activity, maximal drug-mediated activity, drug potency, and sensitivity, respectively. As shown in Fig. 7B, prolonged treatment with either agonist resulted in a marked reduction in the ability of CCh to stimulate PI hydrolysis. A one-way ANOVA revealed a significant ($p < 0.05$) decrease in the slope, midpoint location, and maximal asymptote of the curves generated in the agonist-pretreated cells in comparison to the control cells. The degree of reduction in potency and sensitivity of the assay system to CCh, in response to pretreatment with either agonist, was similar ($p > 0.05$; Fig. 7B), whereas the maximal effects of CCh varied with the agonist used. Of particular note is the fact that basal PI levels were not significantly different ($p > 0.05$) across the groups, indicating that the persistent activating effects of xanomeline are lost on prolonged (24-hr) treatment.

TABLE 2

Activation of PI hydrolysis in CHO hm1 cells by CCh and xanomeline in the absence and presence of atropine (30 nM)

PI hydrolysis was measured over 1 hr at 37° in HEPES buffer, as described in the text. Parameters derived from computer-assisted nonlinear regression analysis are presented as the mean ± standard error of five determinations conducted in triplicate. The basal curve parameter was constrained to 0 for the analysis.

Agonist	CCh[a]	Xanomeline[b]
E_{max}[c]	96 ± 7	Control 95 ± 7 +Atropine 92 ± 6
pEC_{50}	Control 5.66 ± 0.04 +Atropine 4.29 ± 0.06	Control 7.78 ± 0.17 +Atropine 6.79 ± 0.06
n_H[d]	1.24 ± 0.07	Control 0.92 ± 0.13 +Atropine 1.21 ± 0.16
Fold-shift[e]	21.4 ± 2.2	13.5 ± 2.3

[a] Results shown are from constrained, simultaneous nonlinear regression analysis using SCIENTIST.

[b] Student's t test found a significant ($p < 0.05$) difference between control and atropine-treated groups. Accordingly, constrained simultaneous analysis was not performed. Results shown are from standard nonlinear regression analysis using PRISM.

[c] Expressed as percentage of the control CCh maximum response (7500 ± 800 dpm).

[d] Logistic slope factor.

[e] Geometric mean of the ratio of EC_{50} in the presence of antagonist to EC_{50} in the absence of antagonist, determined in each individual experiment.

Effect of atropine on xanomeline-pretreated cells. We demonstrated previously that coincubation of CHO hm1/nNOS cells with both xanomeline (1 μM) and the antagonist atropine (10 μM) during the 1- hr pretreatment phase abolished the ability of xanomeline after its washout to enhance basal nNOS activity, suggesting a receptor-specific mechanism (Christopoulos and El-Fakahany, 1997). In the current study, this interaction was investigated further. Cells were allowed to incubate for 1 hr with 1 μM xanomeline in the absence of atropine and subsequently were washed extensively and assayed for basal L-[^{3}H]citrulline formation in the absence or presence of atropine (10 μM). As shown in Fig. 8, the subsequent addition of atropine to xanomeline-pretreated cells resulted in a significant ($p < 0.05$) reduction in the ability of xanomeline to persistently activate the receptor, suggesting an apparent competitive interplay between the two agents at the M_1 mAChR. In a parallel series of experiments, cells were preincubated with xanomeline for 1

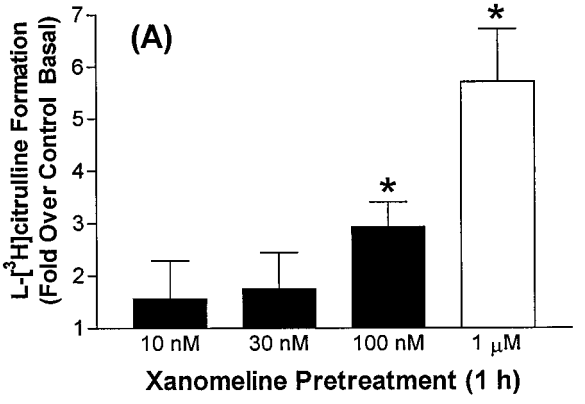

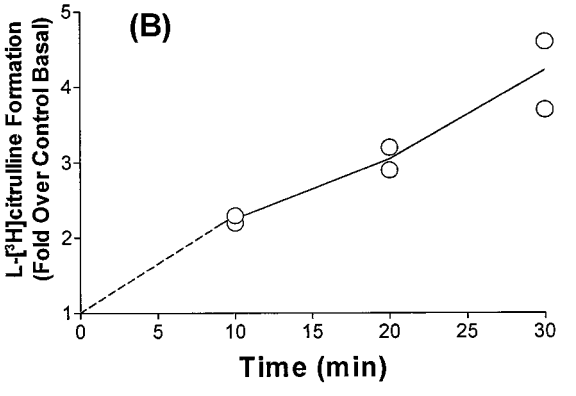

Fig. 6. Effects of xanomeline pretreatment, followed by washout, on basal nNOS activity in CHO hm1/nNOS cells. A, Concentration dependence. Cells were incubated with the indicated concentrations of xanomeline for 1 hr at 37° before harvesting, washing (three times), and assaying the conversion of L-[^{3}H]arginine to L-[^{3}H]citrulline, as described in the text. Basal activity in control cells was 3600 ± 1100 dpm. *Open bar*, results from our previous study (Christopoulos and El-Fakahany, 1997) for comparison. A one-way ANOVA detected a significant difference ($p < 0.05$) between the indicated (*) pretreated cell groups compared with controls. *Bars*, mean ± standard error of five independent experiments conducted in quintuplicate. B, Time dependence. Cells were incubated with 1 μM xanomeline for the indicated times before harvesting and assaying, as above. A significant difference ($p < 0.05$) was noted for enzyme activity at all time periods compared with control. Values represent two independent experiments conducted in quintuplicate.

hr, followed by the addition of atropine for an additional 1 hr. After extensive washout, the persistent xanomeline effect was reestablished (Fig. 8, *third bar*).

Effects of xanomeline pretreatment on the saturation binding of [^{3}H]NMS. The results of the functional assays indicated a mechanism of interaction of xanomeline that displayed elements of both competitive and noncompetitive, or at least surmountable and insurmountable, behavior. Radioligand binding studies were undertaken to probe more directly the nature of the interaction between xanomeline, the M_1 mAChR, and classic muscarinic ligands. Initially, CHO hm1 cells were subjected to the same pretreatment schedule as used in the functional assays (i.e., 1-hr incubation at 37° with either 1 mM CCh or 1 μM xanomeline, followed by extensive washout). The subsequent ability of a saturating concentration (2 nM) of the classic antagonist [^{3}H]NMS to bind to the M_1 mAChR in agonist-pretreated cells was compared, in parallel, with that in vehicle-pretreated cells. Fig. 9A shows that pretreatment with xanomeline resulted in a significant reduction ($p < 0.05$) in the ability of [^{3}H]NMS to bind to the M_1 mAChR. In contrast, pretreatment with CCh resulted in radioligand binding that was indistinguishable from that observed in controls. The effects on [^{3}H]NMS binding observed in this type of study, however, may have been due to either persistent competition between xanomeline and the radioligand or xanomeline-induced receptor internalization. To distinguish between the two possibilities, complete saturation binding isotherms were established for [^{3}H]NMS in control and xanomeline-pretreated cells. As indicated in Fig. 9B, xanomeline caused a significant ($p < 0.05$) reduction in radioligand affinity (pK_D = 9.86 ± 0.20 for vehicle versus 9.58 ± 0.12 for xanomeline-pretreated cells) with no significant alteration ($p > 0.05$) in maximal cell-surface receptor density (B_{max} = 979 ± 157 fmol/mg protein for vehicle versus 915 ± 130 fmol/mg protein for xanomeline-pretreated cells; four experiments). Thus, xanomeline pretreatment resulted in a 2-fold displacement of the [^{3}H]NMS concentration-occupancy curve. If a competitive interaction is assumed, then an approximate calculation of the residual xanomeline concentration in the receptor compartment may be made using the following linear metameter of the Schild equation (Arunlakshana and Schild, 1959): fold-shift = 1 + [X]/K_X, where [X] is the residual concentration of xanomeline, and K_X is the xanomeline-receptor dissociation constant. Using a value of 30 nM for K_X, as determined in the competition binding assays (see below), yields a value of 30 nM for [X].

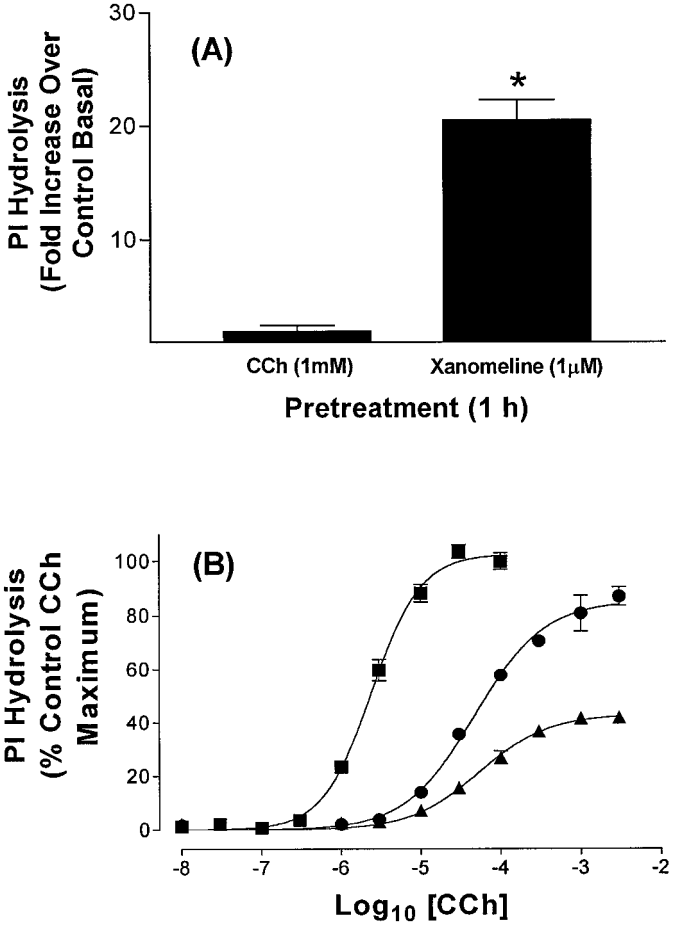

Fig. 7. Effects of agonist pretreatment, followed by washout, on PI hydrolysis in CHO hm1 cells. A, Effects of 1-hr pretreatment, followed by washout, on basal PI activity. Cells were incubated with the indicated concentrations of drugs at 37° before harvesting, washing (three times), and assaying, as described in the text. Basal activity in control cells was 47 ± 10 dpm. A one-way ANOVA revealed a significant difference ($p < 0.05$) between the xanomeline (*)-pretreated cell group compared with controls and CCh-pretreated groups. *Bars*, mean ± standard error of three independent experiments conducted in quintuplicate. B, Effects of 24-hr agonist pretreatment, followed by washout, on CCh-stimulated PI hydrolysis. Cells were incubated at 37° with vehicle (■), 1 mM CCh (▲), or 1 μM xanomeline (●) before harvesting and washing. Cells were then exposed to increasing concentrations of CCh for 1 hr, as described in the text. Results are expressed as percentages of the maximum CCh-induced PI response in control cells (5700 ± 1000 dpm). One-way ANOVA detected significant differences ($p < 0.01$) for midpoint location and slope parameters between control and agonist-pretreated cells but not between the agonist-pretreated cells. Significant differences ($p < 0.01$) were noted, however, between all maximal asymptote parameters. No differences ($p > 0.05$) were found between basal PI levels. Values represent the mean ± standard error of four independent experiments conducted in triplicate. Where error bars are not shown, they lie within the dimensions of the symbol.

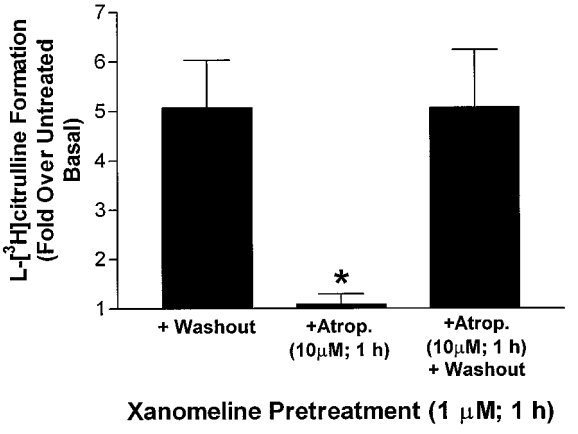

Fig. 8. Effect of atropine on nNOS activity in xanomeline-pretreated and washed CHO hm1/nNOS cells. Cells were incubated with 1 μM xanomeline for 1 hr at 37° before harvesting, washing (three times), and assaying the conversion of L-[^{3}H]arginine to L-[^{3}H]citrulline, as described in the text, in the absence (*first bar from left*) or presence (*center bar*) of 1 μM atropine. The addition of atropine (*Atrop.*) resulted in a significant (*, $p < 0.01$) reduction in persistent xanomeline-mediated nNOS activation. Pretreatment with xanomeline for 1 hr, followed by the addition of atropine for an additional 1 hr before washout, resulted in reestablishment of the xanomeline effect (*third bar from left*). Basal activity in control cells was 6200 ± 1500 dpm. Values represent mean ± standard error of four independent experiments conducted in quintuplicate.

Inhibition by CCh, xanomeline, and atropine of [^{3}H]NMS binding. The concentration-occupancy relationship of xanomeline and its interaction with atropine at the M_1 mAChR were studied indirectly by using a variety of [^{3}H]NMS competition binding assays, conducted over 1 hr at 37° in CHO hm1 cells. Under standard assay conditions (0.2 nM [^{3}H]NMS, approximate K_D concentration), xanomeline was a potent inhibitor of radioligand binding (Fig. 10A). Nonlinear regression analysis yielded parameter estimates that did not seem to deviate from simple competition between the two ligands at a single binding site, with a calculated xanomeline affinity of ~30 nM (Table 3). For the sake of comparison, the effects of CCh (Fig. 10A, Table 3) and atropine (Fig. 10B) also were examined under similar conditions. Unlike xanomeline, CCh displayed a shallow concentration-occupancy relationship, with the midpoint slope significantly less than unity ($p < 0.05$), and seemed to recognize both high (6 μM) and low (178 μM) affinity states of the receptor. In contrast, atropine seemed to interact with a single binding site characterized by a dissociation constant of ~3 nM. Identical patterns of radioligand inhibition were observed in experiments using cell homogenates (data not shown), indicating that agonist-induced desensitization was not a contributing factor to the competition binding curve profile in the intact cells.

A common feature of noncompetitive interactions between multiple ligands at a receptor, however, is that they may not be detected at low concentrations of radioligand but tend to become more evident as higher concentrations of the latter are used (Lee and El-Fakahany, 1991). Thus, competition experiments also were conducted between xanomeline and 2 nM [^{3}H]NMS (Fig. 10A, Table 3). Even in the presence of a 10-fold-higher concentration of [^{3}H]NMS, the binding of xanomeline did not seem to deviate from competitive, surmountable behavior, displaying a characteristic parallel, dextral shift in its competition binding isotherm. Neither the calculated affinity nor the slope factor for the interaction of

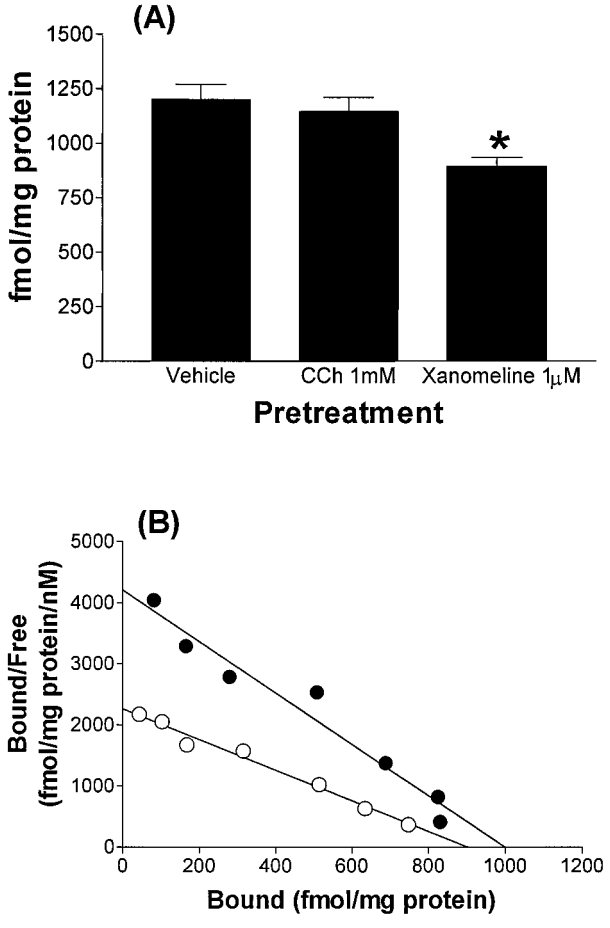

Fig. 9. Effects of agonist pretreatment, followed by washout, on [^{3}H]NMS binding in CHO hm1 cells. A, Cells were incubated with the indicated concentrations of drugs for 1 hr at 37° before harvesting, washing (three times), and subsequent incubation with 2 nM [^{3}H]NMS for 1 hr at 37°. A significant reduction (*, $p < 0.05$) in control radioligand binding (1200 ± 70 fmol/mg protein) was found for the xanomeline-pretreated group. Values represent mean ± standard error of four independent experiments conducted in quintuplicate. B, Scatchard plots for [^{3}H]NMS binding in vehicle (●) and xanomeline (1 μM, 1 hr, 37°)-pretreated (○) cells. Nonlinear regression analysis of the untransformed data revealed a significant difference ($p < 0.05$) between pK_D, but not B_{max}, parameters. Nonspecific binding was defined by 10 μM atropine. Values represent the mean of four independent experiments conducted in triplicate.

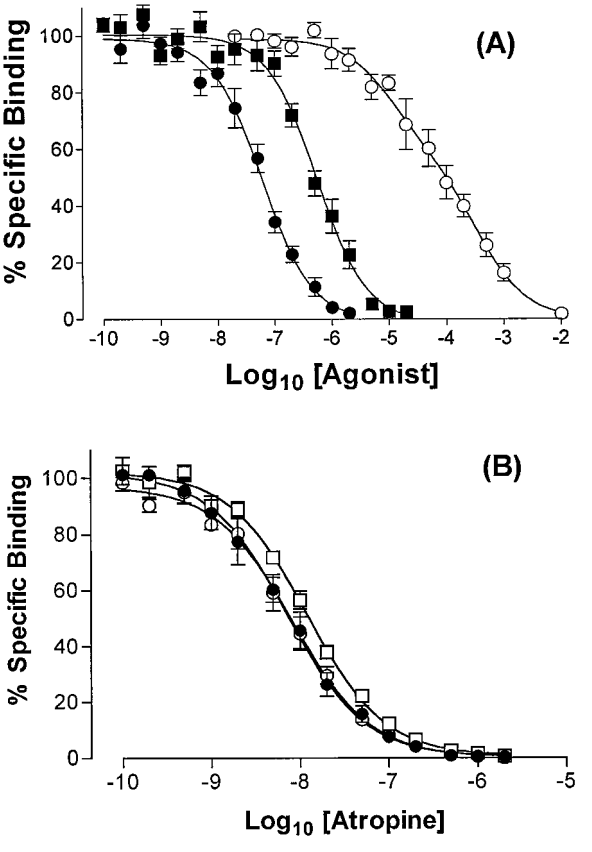

Fig. 10. Inhibition of [^{3}H]NMS binding by CCh, xanomeline, and atropine in CHO hm1 cells. A, Binding isotherms for CCh (○) or xanomeline (●) against 0.2 nM [^{3}H]NMS or xanomeline (■) against 2 nM [^{3}H]NMS. Cells were incubated with drugs for 1 hr at 37°. Nonlinear regression analysis indicated a significantly better fit ($p < 0.05$) of the CCh data to a two-site model, whereas xanomeline seemed to interact with a single class of binding sites with a similar calculated affinity that was independent of radioligand concentration. B. Binding isotherms for atropine against 0.2 nM [^{3}H]NMS (●), 0.4 nM [^{3}H]NMS plus 30 nM xanomeline (○), or 0.6 nM [^{3}H]NMS + 100 nM xanomeline (□). Incubation was for 1 hr at 37°. Nonlinear regression analysis found the data to be best described by a single-site binding model, with affinity estimates for atropine that were not significantly different ($p > 0.05$) from each other under any of the experimental conditions used. Nonspecific binding was defined by 10 μM atropine. Values represent the mean ± standard error of three experiments conducted in triplicate. Where error bars are not shown, they lie within the dimensions of the symbol.

xanomeline with the receptor under these conditions was significantly different ($p > 0.05$) from those determined in the presence of 0.2 nM [^{3}H]NMS (Table 3).

The findings in the functional assays with atropine, however, prompted further competition binding assays, in which the ability of the antagonist to inhibit the binding of varying concentrations of [^{3}H]NMS was studied in the concomitant presence of increasing concentrations of xanomeline (Fig. 10B, Table 3). If the ligands were acting noncompetitively in a concentration-dependent manner, then deviations should be noted in the binding profile of atropine in the presence of xanomeline. However, as may be seen in Table 3, the apparent affinity of atropine for the M_1 mAChR did not change significantly ($p > 0.05$) under any of the assay conditions, provided the occupancy of the receptor by both the radioligand and xanomeline were accounted for (see Experimental Procedures). These findings are in contrast to the suggestion of noncompetitivity for the interaction between xanomeline and atropine at the M_1 mAChR in the functional assays.

Effects of xanomeline on [^{3}H]NMS dissociation. Noncompetitive interactions can alter receptor conformation such that the dissociation characteristics of the radioligand also would change (Lazareno and Birdsall, 1995; Kostenis and Mohr, 1996). Therefore, radioligand kinetic experiments were undertaken in CHO hm1 cells to determine the dissociation rate constant (k_{off}) of [^{3}H]NMS in the absence and presence of a high concentration (1 μM) of xanomeline. After a 1-hr radioligand/receptor equilibration period at 37°, dissociation was promoted by isotopic dilution with 200 nM of unlabeled NMS. In each instance, radioligand dissociation was better described by a monoexponential model, as determined by Prism. As may be seen in Fig. 11A, the presence of xanomeline had no significant effect ($p > 0.05$) on [^{3}H]NMS dissociation, with the k_{off} values being 0.25 ± 0.03 and 0.23 ± 0.05 min^{-1} in the absence and presence of xanomeline, respectively. To discount the possibility that any effects of xanomeline on the dissociation characteristics of [^{3}H]NMS were not evident due to slow xanomeline kinetics at [^{3}H]NMS-occupied receptors, additional experiments were conducted using cells that were preequilibrated with both [^{3}H]NMS (0.4 nM) and xanomeline (30 nM) before promotion of radioligand dissociation. Even under these conditions, the presence of xanomeline (1 μM final concentration) resulted in no significant ($p > 0.05$) alteration of radioligand dissociation rate (k_{off} = 0.34 ± 0.05 min^{-1}), providing further evidence for a competitive interaction at the classic ligand binding site.

Effects of order of ligand addition on attainment of [^{3}H]NMS equilibrium binding. If the persistent mechanism of xanomeline binding involved interaction with a significant subset of attachment points on the receptor shared by classic muscarinic ligands, then this would be expected to result in significantly different degrees of reduced radioligand binding at equilibrium, dependent on the order of ligand addition. This latter possibility was assessed by allowing CHO hm1 cells to incubate with 2 nM [^{3}H]NMS for 2.5 hr at 37° in the absence or presence of either 100 μM CCh or 100 nM xanomeline, added together with, 30 min before, or 30 min after the radioligand. Fig. 11B summarizes the results of these experiments, in which it may be seen that the control level of [^{3}H]NMS binding (598 ± 28 fmol/mg protein) was reduced to a similar extent by either agonist regardless of the order of addition.

Discussion

In agreement with previous reports (Shannon *et al*., 1994), the current study has identified xanomeline as a potent M_1 agonist in functional assays of nNOS activation and PI hydrolysis (Figs. 2 and 3). Furthermore, the very steep slopes associated with both CCh and xanomeline-mediated nNOS activation (Fig. 2, Table 1) are indicative of an exquisite degree of sensitivity of the transduction pathways within the CHO hm1/nNOS cells in the generation of the this response in comparison to agonist-mediated PI hydrolysis (Fig. 3, Table 1). This is consistent with the known, nonlinear dependence of the former biochemical process on the latter (Wang *et al*., 1994). However, the persistent nature of the interaction of xanomeline with the mAChR, as well as the reduced potency of atropine and pirenzepine in functionally antagonizing the effects of xanomeline compared with CCh, are novel findings that have significant implications in terms of understanding alternate modes of mAChR activation and therapeutic use of xanomeline. The results of the current study investigating these phenomena may be summarized as follows: (1) a fraction of added xanomeline, unlike CCh, is resistant to extensive washout and persists within the receptor compartment to exert an agonistic effect; (2) this effect seems to be concentration dependent and is manifested within a 10-min contact time of agent with receptor before washout; (3) the phenomenon transcends the type of experimental assay used; (4) the effect is susceptible to reversal by atropine but is reestablished on removal of atropine; (5)

TABLE 3

Comparison of ligand binding properties of CCh, xanomeline and atropine in CHO hm1 cells

Competition binding experiments were conducted for 1 hr at 37° in HEPES buffer as outlined in the text. Parameters derived from nonlinear regression analysis are presented as the mean ± standard error of three determinations conducted in triplicate.

Competitor	[^{3}H]NMS	[Xanomeline]	pK_H[a]	pK_L[b]	pK_I[c]	n_H[d]
	nM	nM				
CCh	0.2		5.25 ± 0.15 (40.8%)	3.75 ± 0.13		0.56 ± 0.08[e]
Xanomeline	0.2				7.51 ± 0.03	0.92 ± 0.11
	2				7.38 ± 0.09	1.02 ± 0.14
Atropine	0.2				8.50 ± 0.15	0.94 ± 0.08
	0.4	30			8.75 ± 0.07	0.97 ± 0.08
	0.6	100			8.64 ± 0.07	0.94 ± 0.07

[a] Negative logarithm of the dissociation constant for the high affinity agonist binding site; percentage of binding sites is given in parentheses.
[b] Negative logarithm of the dissociation constant for the low affinity agonist binding site.
[c] Negative logarithm of the dissociation constant for binding to a single affinity site, calculated as described in Experimental Procedures.
[d] Logistic slope factor.
[e] Significantly different from unity.

whereas the interaction of xanomeline with the M_1 mAChR seems to be largely competitive, certain elements of this interaction are not completely compatible with simple, surmountable competition.

Persistent increases in basal M_1 mAChR-mediated nNOS activity and PI hydrolysis were observed after short term incubation of CHO cells with xanomeline (Figs. 6A and 7A). However, increasing the pretreatment time to 24 hr resulted in a return of basal PI hydrolysis to control levels (Fig. 7B).

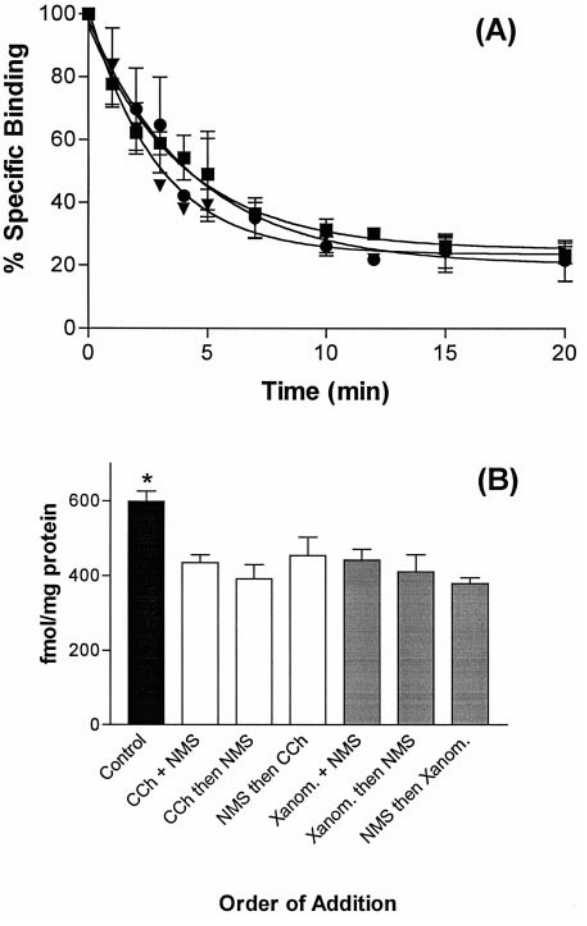

Fig. 11. Lack of xanomeline effect and order of ligand addition on the dissociation kinetics and time to attainment of steady state binding levels of [^{3}H]NMS, respectively. A, ■, Time course of dissociation of 0.2 nM [^{3}H]NMS in the presence of 200 nM unlabeled NMS. ●, Time course of dissociation of 0.2 nM [^{3}H]NMS in the presence of 200 nM unlabeled NMS plus 1 μM xanomeline; ▼, Time course of dissociation of 0.4 nM [^{3}H]NMS (preincubated with 30 nM xanomeline for 1 hr) in the presence of 200 nM unlabeled NMS plus 1 μM xanomeline. The latter paradigm was used to discount the possibility that the lack of xanomeline effect on radioligand dissociation kinetics was due to slow xanomeline binding kinetics at radioligand-occupied receptors. Monoexponential dissociation rate constants were calculated via nonlinear regression analysis, with no significant difference ($p > 0.05$) between any of the treatments. Values represent the mean of three independent experiments conducted in duplicate. Where error bars are not shown, they lie within the dimensions of the symbol. B, Effects of 100 μM CCh (*open bars*) or 100 nM xanomeline (*shaded bars*) on the equilibrium level of binding of 2 nM [^{3}H]NMS. Where a sequential order of addition is indicated, the first-mentioned ligand was added to the cells 30 min before the second-mentioned ligand, and both were subsequently allowed to incubate for an additional 2 hr at 37°. Control (*solid bar*) radioligand binding was 597.8 ± 27.5 fmol/mg protein. Agonists significantly reduced (*, $p < 0.05$) control radioligand binding to similar extents, with no significant differences ($p > 0.05$) between the various treatment regimens. Nonspecific binding was defined by 10 μM atropine. Values represent the mean of three independent experiments conducted in quintuplicate.

This implies that despite being able to activate the receptor in a persistent manner, the xanomeline effect eventually succumbs to the desensitization machinery of the intact cell, a feature common to the majority of agonist-induced responses in physiological systems (Nathanson, 1989; Lohse, 1993). The results shown in Fig. 7B also indicate that xanomeline induced a significantly lower degree of system desensitization than did CCh, under conditions of approximate receptor-occupancy equivalence with respect to pretreatment concentration (~20 × IC_{50} value, Fig. 10A). The ability of agonists to induce desensitization may be correlated with their efficacy (Hu *et al.*, 1991; January *et al.*, 1997); hence, our findings with xanomeline tend to support previous claims that this agent is actually a partial agonist (Shannon *et al.*, 1994). In addition, the competition binding experiments also support this conclusion because CCh, but not xanomeline, yielded a biphasic competition binding curve (Fig. 10A). As with the ability to induce desensitization, deviations from monophasic competition binding at a single receptor subtype also may be related to the efficacy of the agonist, being less pronounced with partial agonists in comparison to full agonists (Zhu *et al.*, 1994). The loss of the persistent activating effect of xanomeline after prolonged (24-hr) treatment may simply be a reflection of the fact that given sufficient time, partial agonists also may induce desensitization of their own agonistic effects, especially if used in high concentrations (Hu *et al.*, 1991).

The simplest explanation to account for the persistent activating effects of xanomeline relates to the lipophilic nature of the compound. The aliphatic hexyloxy side chain (Fig. 1) may be predicted to contribute to the ability of this compound to partition indiscriminately into biological membranes, resulting in the development of a substantial depot of agonist that can demonstrate relative resistance to washing. However, three experimental observations point to a more specific receptor-mediated mechanism of interaction that can account for the effects of xanomeline. First, our previous demonstration that coincubation of xanomeline with atropine in the pretreatment phase prevents the ability of the former agent to display persistent receptor activation (Christopoulos and El-Fakahany, 1997). This suggests that a prerequisite for the establishment of the phenomenon is the ability of xanomeline to gain access to regions on the receptor that are also used by atropine. Second, the reappearance of the residual agonistic activity of xanomeline, after washout of atropine (Fig. 8), suggests that the persistent binding of xanomeline occurs in regions of close proximity to the receptor. Third, the lipophilicity of this compound may actually result in a significant degree of its depletion at the level of the receptor compartment. Functionally, this would be manifested as an increased potency of a competitive antagonist in the inhibition of xanomeline-mediated responses compared with responses elicited by a hydrophilic agonist, such as CCh. As shown in Figs. 4 and 5 and Tables 1 and 2, however, in neither type of functional assay did atropine or pirenzepine seem to be better able to inhibit the responses to xanomeline relative to those of CCh. In fact, the opposite was observed. This supports the hypotheses that the interaction between xanomeline and atropine involves a receptor-mediated mechanism and that this mechanism is different in nature from that between atropine and CCh.

Although the above considerations point to a receptor-specific mechanism to account for the persistent actions of

xanomeline, aspects of the functional assays suggest that this mechanism may be noncompetitive in nature when assessed in terms of the interaction between xanomeline and atropine. This was particularly evident in the PI assay, in which significant differences in xanomeline concentration-response curve shape were detected in the absence and presence of atropine. Furthermore, the antagonist exhibited a reduced potency in inhibiting xanomeline-mediated responses in comparison to CCh-mediated responses (Fig. 5). Theoretically, the magnitude of the shift that a competitive antagonist is able to produce on an agonist concentration-response curve should be independent of the potency and efficacy of the agonists used, provided these agonists activate the response via the same receptor (Kenakin, 1997). The reduced potency of atropine in inhibiting xanomeline-mediated responses, relative to CCh-mediated responses, cannot be attributed to M_1-independent receptor-activating properties of xanomeline because no responses to this agent were observed in nontransfected CHO cells (data not shown). Thus, it is possible that the persistent nature of xanomeline binding introduces additional steric or conformational effects that confound the ability of antagonists to bind. However, the unambiguous assignment of a noncompetitive mode of interaction between agonist/antagonist pairs would require a more rigorous pharmacological analysis, using a range of antagonist concentrations, than that undertaken in the current study. Furthermore, it is quite possible that the differential abilities of CCh and xanomeline to desensitize the M_1 mAChR also may contribute to the apparent noncompetitive interaction observed in the functional assays, not by altering antagonist binding properties but instead by changing the agonist concentration-response relationship at the higher agonist concentrations that are required to overcome the antagonism by atropine.

A number of radioligand binding paradigms were used to assess further the mechanism or mechanisms of interaction of xanomeline with the M_1 mAChR. Increasing the [^{3}H]NMS concentration 10-fold resulted in a parallel, dextral shift of the xanomeline competition curve (Fig. 10A), with complete inhibition of radioligand binding still achievable. Such a profile is predicted for competitive interactions, in contrast to noncompetitive interactions that deviate from this behavior when progressively higher radioligand concentrations are used (Lee and El-Fakahany, 1991). Furthermore, the affinity of xanomeline, calculated with the assumption of competition, was not significantly different in either instance, demonstrating the independence of this characteristic drug/receptor parameter from radioligand concentration. Ligand-induced conformational changes also may be detected as alterations of radioligand dissociation rate in the presence of a modulating agent (Lee and El-Fakahany, 1991; Lazareno and Birdsall, 1995; Kostenis and Mohr, 1996). Again, this possibility was not substantiated in the dissociation kinetic experiments (Fig. 11A), in which the control radioligand dissociation rate was unaltered by the presence of xanomeline. If the mechanism of interaction involved an essentially pseudoirreversible steric phenomenon, such as a persistent "capping" of the classic ligand binding site, then the order of ligand addition would be expected to result in differing degrees of steady state binding (Proška and Tucek, 1994). This was not observed; the combination of both xanomeline and [^{3}H]NMS resulted in similar levels of steady state binding, regardless of the order of addition (Fig. 11B). Finally, if the interaction were noncompetitive only between the specific combination of atropine and xanomeline, then the [^{3}H]NMS/xanomeline/atropine competition experiments (Fig. 10B) should have provided some evidence for this phenomenon, yet none was noted (Table 3).

A finding consistent with a competitive mode of interaction between residual xanomeline and other ligands at the classic binding site on the mAChR also was observed in the [^{3}H]NMS saturation binding experiments (Fig. 9), in which pretreatment with xanomeline, followed by washout, affected apparent radioligand binding affinity but not maximal receptor density. As calculated from Fig. 9B, pretreatment with 1 μM xanomeline, followed by extensive washout, resulted in the equivalent of ~3.3% of the added xanomeline displaying a tenacious binding ability. Furthermore, the calculated residual concentration of 30 nM is sufficient to account for the elevation of basal response to near-maximal levels of receptor activation (Figs. 6A and 8), as determined by inspection of the complete xanomeline concentration-response curves in the L-[^{3}H]citrulline assay (Figs. 2 and 4). At this point, it is worth noting that the residual concentration and, indeed, calculated affinity constants for xanomeline determined in this study are, quite possibly, composite measures, with their true values being dictated by the relative contributions of both reversible and pseudoirreversible binding components. At the very least, however, they may still be used as empirical descriptors of the overall binding phenomenon.

While attempting to construct an explanatory scheme that encompasses our experimental findings, it is evident that much of the behavior exhibited by xanomeline is reminiscent of observations made with the β_2-adrenoceptor agonist salmeterol (Coleman *et al.*, 1996). The latter compound has been studied extensively due to its ability to display persistent binding and an extremely long duration of action (Nials *et al.*, 1993). To explain the findings with salmeterol, an "exosite" model has been postulated, in which the lipophilic phenylalkyloxalkyl "tail" of the compound attaches itself to a complementary region on the receptor, distinct from the classic agonist binding site, in a pseudoirreversible manner (Green *et al.*, 1996), whereas the saligenin "head" of the compound interacts in a reversible manner with the classic site to activate the receptor. However, the study of the interaction between salmeterol or xanomeline with competitive antagonists also points to important differences between the two agonists. Radioligand binding experiments with salmeterol have suggested a pseudoirreversible mechanism of attachment, whereas functional experiments were consistent with surmountable competition (Nials *et al.*, 1993; Clark *et al.*, 1996). Conversely, xanomeline seemed competitive in binding assays, as reported herein. In addition, coincubation of salmeterol with competitive antagonists did not prevent the establishment of a persistent receptor-activating effect of the agonist after antagonist washout (Clark *et al.*, 1996). This latter finding is in contrast to our observations with xanomeline and atropine coincubation followed by washout (Fig. 8), in which the residual agonistic effects of xanomeline reappeared. Thus, although our data suggest that xanomeline may be interacting with an exosite on the M_1 mAChR, the mechanism of binding most likely involves regions of the receptor in a closer spatial proximity to attachment points used by classic antagonists than does the mechanism for

salmeterol at the β_2-adrenoceptor. A possible scheme for xanomeline binding to the M_1 mAChR is depicted in Fig. 12. Salient features of this model include the ability of a large fraction of added xanomeline to interact in a readily reversible manner with the classic agonist binding site, while a minor fraction is able to interact in an orientation that allows persistent binding, yet does not preclude access to the classic site. Competitive antagonists would be expected to interfere predominantly with binding at the classic site but may still sterically hinder interaction at the accessory site. Alternatively, the second binding site may represent a point of attachment only, with the activating effect achievable only on agonist dissociation from the exosite to rebind at the classic site. A third possibility is that the interaction of xanomeline may involve a two-step binding process, in which the agonist first associates with the classic binding site before forming a tighter association with an accessory site. Each of these suggested schemes accommodates the observed effects of atropine. An additional scheme that takes into account the possibility of multiple receptor conformational states (Kenakin, 1997) is that the persistent activating effects of xanomeline are manifested only when the receptor is not "held" in an inactive conformation by antagonists. By proposing such models, we by no means reject the possibility of alternative explanations, nor do we suggest that the orientations of xanomeline depicted in Fig. 12 represent those achieved in the interaction of this agent with the receptor. Obviously, further detailed investigation is warranted. One approach may entail the use of receptor solubilization because the removal of the receptor from its native lipid environment may shed some light on the contribution of the latter to the mechanism of action of xanomeline.

Regardless of the molecular nature of the interaction of xanomeline with the M_1 mAChR, however, the results reported in the current study point to a novel mode of receptor activation that outlasts the presence of free agonist in the receptor compartment. These findings might have significant clinical implications, especially in the treatment of Alzheimer's disease, because the therapeutic and/or side effects of xanomeline may not necessarily be predicted by the measurement of free drug concentration in the cerebrospinal fluid.

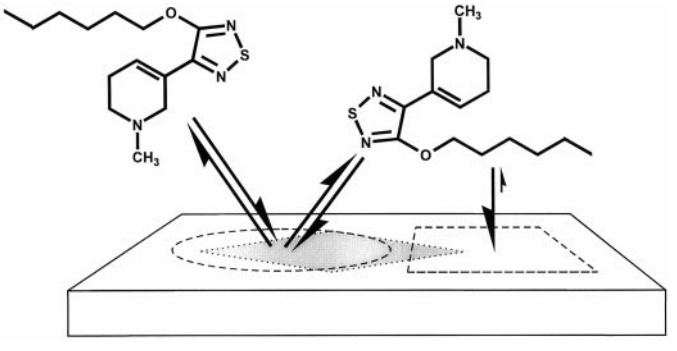

Fig. 12. Suggested scheme of interaction of xanomeline with the M_1 mAChR. *Dashed circle*, receptor domains involved in the binding of classic muscarinic agonists, as well as xanomeline. *Dashed square*, additional binding domains used by xanomeline (but not classic ligands) in its persistent attachment to the receptor. *Shaded diamond*, domains recognized by competitive antagonists such as atropine.

References

Arunlakshana O and Schild HO (1959) Some quantitative uses of drug antagonists. *Br J Pharmacol* **14:**48–58.

Bodick NC, Offen WW, Levey AI, Cutler NC, Gauthier SG, Satlin A, Shannon HE, Tollefson GD, Rasmussen K, Bymaster FP, Hurley DJ, Potter WZ, and Paul SM (1997) Effects of xanomeline, a selective muscarinic receptor agonist, on cognitive function and behavioural symptoms in Alzheimer's disease. *Arch Neurol* **54:**465–473.

Bradford M (1976) A rapid and sensitive method for the quantitation of microgram quantities of protein utilizing the principle of protein-dye binding. *Annal Biochem* **72:**248–254.

Bredt DS and Snyder SH (1989) Nitric oxide mediates glutamate-linked enhancement of cGMP levels in the cerebellum. *Proc Natl Acad Sci USA* **86:**9030–9033.

Bymaster FP, Whitesitt CA, Shannon HE, DeLapp N, Ward JS, Calligaro DO, Shipley LA, Buelke-Sam JL, Bodick NC, Farde L, Sheardown MJ, Olesen PH, Hansen KT, Suzdak PD, Swedberg MDB, Sauerberg P, and Mitch CH (1997) Xanomeline: a selective muscarinic agonist for the treatment of Alzheimer's disease. *Drug Dev Res* **40:**158–170.

Christopoulos A and El-Fakahany E (1997) Novel persistent activation of muscarinic M_1 receptors by xanomeline. *Eur J Pharmacol* **334:**R3–R4.

Clark RB, Allal C, Friedman J, Johnson M, and Barber R (1996) Stable activation and desensitization of β_2-adrenergic receptor stimulation of adenylyl cyclase by salmeterol: evidence for a quasi-irreversible binding to an exosite. *Mol Pharmacol* **49:**182–189.

Coleman RA, Johnson M, Nials AT, and Vardey CJ (1996) Exosites: their current status, and their relevance to the duration of action of long-acting β_2-adrenoceptor agonists. *Trends Pharmacol Sci* **17:**324–330.

Ferrari-Dileo G, Mash DC, and Flynn, DD (1995) Attenuation of muscarinic receptor-G-protein interaction in Alzheimer disease. *Mol Chem Neuropathol* **24:**69–91.

Giacobini E (1992) Cholinomimetic replacement of cholinergic function in Alzheimer's disease, in *Treatment of Dementias* (Meyer EM, Simpkins JW, Yamamoto J, and Crews FT, eds) pp 19–34, Plenum Press, NY.

Green SA, Spasoff AP, Coleman RA, Johnson M, and Liggett SB (1996) Sustained activation of a G-protein coupled receptor via 'anchored' agonist binding: molecular localization of the salmeterol exosite within the β_2-adrenergic receptor. *J Biol Chem* **271:**24029–24035.

Hu J, Wang SZ, and El-Fakahany EE (1991) Effects of agonist efficacy on desensitization of phosphoinositide hydrolysis mediated by m1 and m3 muscarinic receptors expressed in Chinese hamster ovary cells *J Pharmacol Exp Ther* **257:**938–945.

January B, Seibold A, Whaley B, Hipkin RW, Lin D, Schonbrunn A, Barber R, and Clark RB (1997) β_2-Adrenergic receptor desensitization, internalization, and phosphorylation in response to full and partial agonists. *J Biol Chem* **272:**23871–23879.

Kenakin TP (1997) *Pharmacologic Analysis of Drug-Receptor Interaction*, 3rd ed, Lippincott-Raven, New York.

Kostenis E and Mohr K (1996) Two-point kinetic experiments to quantify allosteric effects on radioligand dissociation. *Trends Pharmacol Sci* **17:**280–283.

Ladner CJ, Celesia GG, Magnuson DJ, and Lee JM (1995) Regional alterations in M_1 muscarinic receptor-G protein coupling in Alzheimer's disease. *J Neuropathol Exp Neurol* **54:**783–789.

Lazareno S and Birdsall NJM (1995) Detection, quantitation, and verification of allosteric interactions of agents with labeled and unlabeled ligands at G protein-coupled receptors: interactions of strychnine and acetylcholine at muscarinic receptors. *Mol Pharmacol* **48:**362–378.

Lee NH and El-Fakahany EE (1991) Allosteric antagonists of the muscarinic acetylcholine receptor. *Biochem Pharmacol* **42:**199–205.

Leff P, Prentice DJ, Giles H, Martin GR, and Wood J (1990) Estimation of agonist affinity and efficacy by direct, operational model fitting. *J Pharmacol Methods* **23:**225–237.

Lohse MJ (1993) Molecular mechanisms of membrane receptor desensitization. *Biochim Biophys Acta* **1179:**171–188.

Mash DC, Flynn DD, and Potter LT (1985) Loss of M2 muscarine receptors in the cerebral cortex in Alzheimer's disease and experimental cholinergic denervation. *Science (Washington D C)* **228:**1115–1117.

Nathanson NM (1989) Regulation and development of muscarinic receptor number and function, in *The Muscarinic Receptors* (Brown JH, ed) pp 419–454, Humana Press, NJ.

Nials AT, Sumner MJ, Johnson M, and Coleman RA (1993) Investigations into the factors determining the duration of action of the β_2-adrenoceptor agonist, salmeterol. *Br J Pharmacol* **108:**507–515.

Proška J and Tucek S (1994) Mechanisms of steric and cooperative actions of alcuronium on cardiac muscarinic receptors. *Mol Pharmacol* **45:**709–717.

Quirion R, Aubert I, Lapchak PA, Schaum RP, Teolis S, Gauthier S, and Araujo DM (1989) Muscarinic receptor subtypes in human neurodegenerative disorders: focus on Alzheimer's disease. *Trends Pharmacol Sci* **10**(suppl.)**:**80–84.

Shannon HE, Bymaster FP, Calligaro DO, Greenwood B, Mitch CH, Sawyer BD, Ward JS, Wong DT, Olesen PH, Sheardown MJ, Swedberg MDB, Suzdak PD, and Sauerberg P (1994) Xanomeline: a novel muscarinic receptor agonist with functional selectivity for M_1 receptors. *J Pharmacol Exp Ther* **269:**271–281.

Wang SZ, Zhu SZ, and El-Fakahany EE (1994) Efficient coupling of m5 muscarinic acetylcholine receptors to activation of nitric oxide synthase. *J Pharmacol Exp Ther* **268:**552–557.

Zhu SZ, Wang SZ, Hu J, and El-Fakahany EE (1994) An arginine residue conserved in most G protein-coupled receptors is essential for the function of the m1 muscarinic receptor. *Mol Pharmacol* **45:**517–523.

Send reprint requests to: Prof. Esam E. El-Fakahany, Division of Neuroscience Research in Psychiatry, Box 392, Mayo Memorial, University of Minnesota Medical School, Minneapolis, MN 55455. E-mail: elfak001@maroon.tc.umn.edu